Bulletin of the Seismological Society of America, Vol. 102, No. 6, pp. 2452–2457, December 2012, doi: 10.1785/0120120044

A Graphical Derivation of the Perpendicular Ray Jacobian

by Daryl Van Vorst, Jean Virieux, and Matthew J. Yedlin

Abstract A graphical derivation of the perpendicular part of the ray Jacobian for planar rays is presented and found to match that derived via paraxial raytracing. The graphical method provides the reader with a clear picture of how the ray Jacobian can be factored (for planar rays), how the perpendicular part arises, and that it is easily computed if the ray paths are known. The Jacobian is incorporated into a transfer function that approximately converts 3D measured data into 2D equivalent data that is useful in 2D full-wave inversions.

Introduction

In the following we present a graphical derivation of the perpendicular component of the 3D ray Jacobian for planar rays. This part of the ray Jacobian describes the out-of-plane spreading associated with a ray and is the only difference between the 2D and 2.5D cases in ray theory (Červený, 2001, pp. 394). The difference between the two cases for full-wave simulations is more complex, but knowledge of the perpendicular component of the Jacobian allows one to preprocess real-world acoustic and ground-penetrating radar data into a form that is usable for 2D full-wave inversion, provided the geology is sufficiently 2.5D.

Planar rays imply that the derivative of velocity in the direction normal to the plane is zero. Here, we satisfy this by assuming that the material properties do not vary normal to the plane, but the arguments are also applicable as long as the normal derivative vanishes. In that case, the velocity does not vary in the direction normal to the plane if one stays in an infinitesimal region near the plane. Previous related work focused on mapping 3D acoustic data to 2D includes that of Červený and Ravindra (1971, pp. 74–93), Červený and Hron (1980), and Bleistein (1986).

The 3D to 2D data transfer function for the acoustic-wave problem derived in Yedlin *et al.* (2012) (see Yedlin, 1987) is

$$TF = \frac{u_{2D}(w)}{u_{3D}(w)} = -i\pi H_0^{(2)}[\omega T(s)]\sqrt{\frac{v(0)J_{3D}(s)T(s)}{\sin(\theta_0)J_{2D}(s)}}e^{i\omega T(s)}. \tag{1}$$

In equation (1), $H_0^{(2)}$ is a Hankel function, $v(0)$ is the velocity at the source, s is the arc length of the ray from source to receiver, $T(s)$ is the travel time from source to receiver, $J_{3D}(s)$ is the 3D Jacobian at the receiver, $J_{2D}(s)$ is the 2D Jacobian at the receiver, and θ_0 is the take-off inclination. The transfer function transforms the measured field, $u_{3D}(w)$, into an equivalent 2D field, $u_{2D}(w)$. Here, and in the rest of the paper, it is assumed that the complex time dependency is $e^{i\omega t}$.

Ray-based inversions usually precede full-wave inversions and provide much of the information that is required to compute equation (1): ray paths and an approximate velocity distribution (travel time is already known from picking first arrivals). In the following we show, through graphical and paraxial methods, that aside from travel time, the remaining quantities in the radical in equation (1) amount to an integral of velocity along a ray.

For both the graphical and paraxial derivations, we assume that the coordinate system has been selected such that the plane where the 2D inversion is to be performed is $y = 0$. When working in 3D, spherical coordinates are used where θ is the inclination, and ϕ is the azimuth. We are interested in how rays behave when very close to the $y = 0$ plane, so the azimuth angle is very small and is represented as $\mathrm{d}\phi$, as indicated in Figures 1 and 2. It is also assumed that the material parameters do not vary as a function of y.

Graphical Derivation of $J^{\perp}$

We begin with the graphical derivation of the ratio of ray Jacobians. First, we show that the 3D ray Jacobian can be factored into a parallel part, $J^{\parallel} = J_{2D}$, and a perpendicular part $J^{\perp}$. Next, a simple expression to compute $J^{\perp}$ is derived with the assumption that the in-plane ray is straight. Finally, it is shown that the expression is valid for curved rays.

Jacobian Factorization

The 3D ray Jacobian, $J_{3D}(s, \theta_0, \phi_0)$, relates the cross-sectional area of the ray tube, $\mathrm{d}S$, to the associated infinitesimal changes in the take-off angles, $\mathrm{d}\theta$ and $\mathrm{d}\phi$:

$$\mathrm{d}S = J_{3D}\mathrm{d}\theta\mathrm{d}\phi. \tag{2}$$

An illustration of the 3D ray Jacobian for a planar ray is shown in Figure 1.

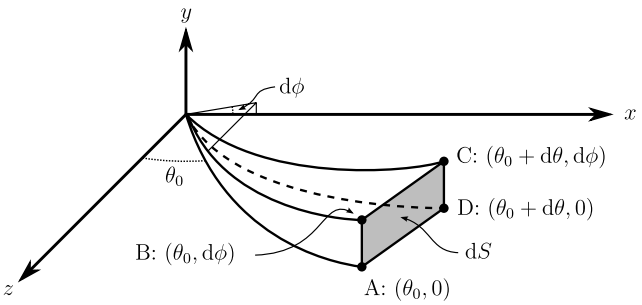

Figure 1. A ray tube cut off at a particular arc length, s. The shaded end with vertices A, B, C, and D corresponds to the area, $\mathrm{d}S = J(s,\theta_0)|_{\phi_0=0}\mathrm{d}\theta\mathrm{d}\phi$, covered by the ray as the take-off angles (θ_0 and $\phi = 0$) are perturbed by $\mathrm{d}\theta$ and $\mathrm{d}\phi$, respectively. The arc from the origin to point A is the original unperturbed ray.

Similarly, the 2D ray Jacobian relates the length of the arc spanned by the end of the ray to a perturbation of the take-off angle, $\mathrm{d}\theta$:

$$\mathrm{d}S_{2D} = J_{2D}\mathrm{d}\theta. \tag{3}$$

In Figure 1 this corresponds to the length of the line segment AD.

To find the relationship between the 2D and 3D Jacobians, it is useful to determine the shape of the surface element $\mathrm{d}S$. This can be accomplished by applying Snell's law to the model. If we approximate the true continuum of velocity with a fine grid of rectangular prisms, each with constant velocity, then we can apply Snell's law directly. The prisms finely discretize the model in the x and z directions (they break up the $y = 0$ plane into small rectangles) and are infinitely long in the y direction, thus maintaining a 2.5D representation of the model. The surface normals of these prisms have no y component because there is no material variation in the y direction. We can apply the vector form of Snell's law,

$$\frac{\hat{\mathbf{t}}_1 \times \hat{\mathbf{n}}}{v_1} = \frac{\hat{\mathbf{t}}_2 \times \hat{\mathbf{n}}}{v_2}, \tag{4}$$

to any interface in this discretization. In equation (4) the velocities on either side of the interface are v_1 and v_2, the unit

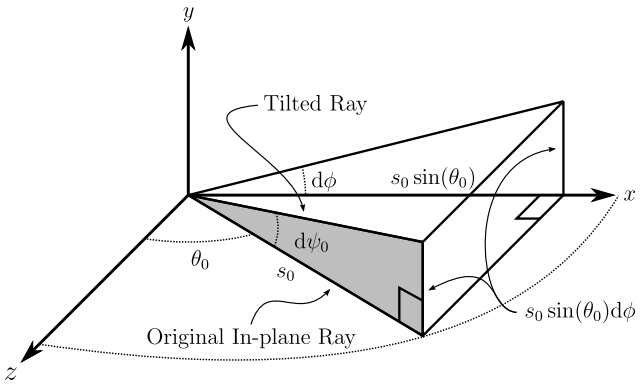

Figure 2. Calculation of the angle, $\mathrm{d}\psi_0$, between the tilted ray segment, with take-off angles θ_0 and $\mathrm{d}\phi$, and its in-plane projection with length s_0. The angle $\mathrm{d}\phi$ is assumed small.

tangent vectors to the ray are $\hat{\mathbf{t}}_1$ and $\hat{\mathbf{t}}_2$, and the surface normal is $\hat{\mathbf{n}}$. The components of $\hat{\mathbf{t}}_1$ or $\hat{\mathbf{t}}_2$ are related to the spherical coordinates θ and ϕ by

$$t_x = \sin(\theta)\cos(\phi), \tag{5}$$

$$t_y = \sin(\theta)\sin(\phi), \tag{6}$$

and

$$t_z = \cos(\theta). \tag{7}$$

Equating the y components of the cross products for small azimuthal angles $\mathrm{d}\phi_1$ and $\mathrm{d}\phi_2$, we have

$$\frac{n_x\cos(\theta_1) - n_z\sin(\theta_1)\cos(\mathrm{d}\phi_1)}{v_1} = \frac{n_x\cos(\theta_2) - n_z\sin(\theta_2)\cos(\mathrm{d}\phi_2)}{v_2}. \tag{8}$$

The angles $\mathrm{d}\phi_1$ and $\mathrm{d}\phi_2$ are infinitesimal because the ray is either in-plane or perturbed only slightly to be out-of-plane, thus allowing us to simplify equation (8):

$$\frac{n_x\cos(\theta_1) - n_z\sin(\theta_1)}{v_1} = \frac{n_x\cos(\theta_2) - n_z\sin(\theta_2)}{v_2} + O(\mathrm{d}\phi_1^2) + O(\mathrm{d}\phi_2^2). \tag{9}$$

In the limit as $\mathrm{d}\phi$ approaches zero, the error terms in equation (9) vanish. For small $\mathrm{d}\phi$, the projection of the ray onto the plane is governed by equation (9). The projection is independent of $\mathrm{d}\phi$ because t_x and t_z only depend on θ. As $\mathrm{d}\phi$ is increased from zero, the ray must therefore lift vertically out of the plane, as indicated by $t_y \approx \sin(\theta)\mathrm{d}\phi$. So the surface element $\mathrm{d}S$ in Figure 1 is indeed a rectangle, and the element area is equal to the product of the lengths of the sides. If there had been a dependency on $\mathrm{d}\phi$ in equation (9), then a change in $\mathrm{d}\phi$ would cause the end of the ray to move at an angle out of the plane, and $\mathrm{d}S$ would no longer be rectangular.

The rectangular nature of $\mathrm{d}S$ allows us to factor the 3D Jacobian and write

$$J_{3D} = J^{\parallel}J^{\perp}, \tag{10}$$

and

$$J_{2D} = J^{\parallel}, \tag{11}$$

where $J^{\parallel}$ is the in-plane (parallel) portion of the 3D Jacobian, and $J^{\perp}$ is the out-of-plane (perpendicular) portion of the 3D Jacobian. Graphically, these components are (referring to Fig. 1),

$$J^{\parallel} = \frac{\text{Length AD}}{\mathrm{d}\theta} = \frac{\text{Length BC}}{\mathrm{d}\theta}, \tag{12}$$

and

$$J^{\perp} = \frac{\text{Length AB}}{\mathrm{d}\phi} = \frac{\text{Length CD}}{\mathrm{d}\phi}. \tag{13}$$

Thus, the ratio of Jacobians in equation (1) simplifies to $J^{\perp}$.

Derivation of $J^{\perp}$ for a Straight Ray

The perpendicular portion of the ray Jacobian, $J^{\perp}$, can be determined geometrically by relating the length of the segment AB to $\mathrm{d}\phi$ (Fig. 1). For simplicity, we depart from the prismatic discretization that we used to demonstrate the factorizability of J_{3D} (equation 10) and compute $J^{\perp}$ for a straight ray (at an arbitrary inclination θ_0). To ensure that the unperturbed in-plane ray is straight, the material must consist of slabs with surface normals parallel to the ray, as shown in Figure 3. In the Extension to Curved Rays section, we show that this result also applies to curved rays through an arbitrary 2.5D medium.

A profile of the ray as it travels through layers of varying velocity is illustrated in Figure 4. The in-plane ray is initially straight (the horizontal axis in the figure) and at normal incidence to each layer. It is then tilted up out of the plane by a small angle, $\mathrm{d}\psi_0$. The gray section in Figure 2 corresponds to the far left layer, v_0, of Figure 4.

From the definition of spherical coordinates, perturbing a point $(s_0, \theta_0, 0)$ by $\mathrm{d}\phi$ to $(s_0, \theta_0, \mathrm{d}\phi)$ results in a displacement $\mathrm{d}y = s_0 \sin(\theta_0)\mathrm{d}\phi$ out of the plane. The displacement is related to an effective angle, $\mathrm{d}\psi_0$, by $\mathrm{d}y = s_0\mathrm{d}\psi_0$. The first ray segment with inclination θ_0 and azimuth perturbation $\mathrm{d}\phi$ makes an angle, $\mathrm{d}\psi_0$, with the $y = 0$ plane (refer to Fig. 2):

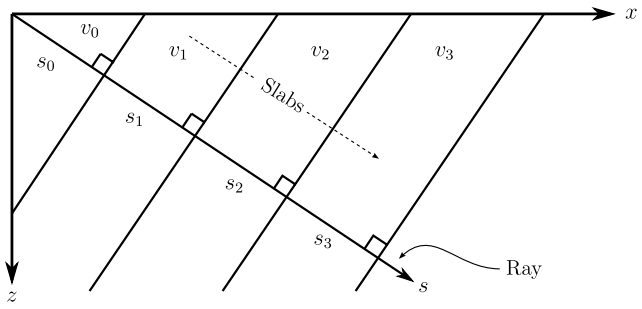

Figure 3. A ray normally incident on a layered structure. Each layer consists of a constant velocity v_i and is of thickness s_i. The total length of the ray is s.

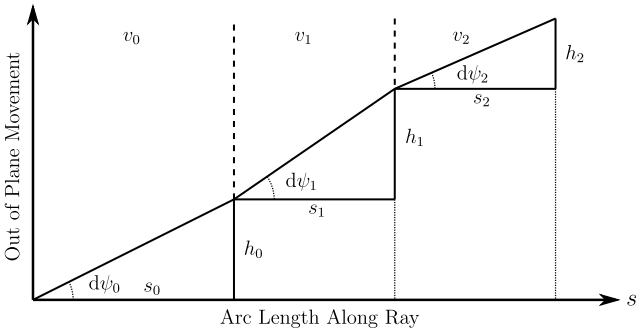

Figure 4. Out-of-plane spreading, h_i, along a ray that is initially straight and normally incident to a layered structure with constant velocities, v_i. The ray is tilted up by a small angle, $\mathrm{d}\psi_0$. Each layer has a thickness, s_i.

$$\mathrm{d}\psi_0 = \sin(\theta_0)\mathrm{d}\phi. \tag{14}$$

This is recognizable as part of the canonical solid-angle $\mathrm{d}\Omega = \sin(\theta)\mathrm{d}\theta\mathrm{d}\phi$ and is the root of the difference between the solid-angle Jacobian, J^{Ω}_{3D}, and the Jacobian, J_{3D}, related to perturbations of the spherical coordinates θ and ϕ.

As the ray travels through the layers of material with velocity v_i, the angle, $\mathrm{d}\psi_i$, that each segment, i, makes with the $y = 0$ plane changes according to Snell's law,

$$\frac{\sin(\mathrm{d}\psi_i)}{v_i} = \frac{\sin(\mathrm{d}\psi_{i+1})}{v_{i+1}}, \tag{15}$$

or

$$\frac{\mathrm{d}\psi_i}{v_i} \approx \frac{\mathrm{d}\psi_{i+1}}{v_{i+1}}, \tag{16}$$

for small angles. This is illustrated in Figure 4.

The elevation of the ray off of the plane increases by an amount h_i as it travels through each layer. For each segment, this elevation is related to the angle $\mathrm{d}\psi_i$ by

$$h_i = s_i \tan(\mathrm{d}\psi_i) \approx s_i \mathrm{d}\psi_i, \tag{17}$$

where s_i is the length of the original ray segment.

Combining equations (17) and (16) and summing gives the total elevation, h, of the ray (segment AB in Fig. 1):

$$h = \sum_{i=0}^{N} h_i \approx \frac{\mathrm{d}\psi_0}{v_0} \sum_{i=0}^{N} s_i v_i = \frac{\sin(\theta_0)\mathrm{d}\phi}{v_0} \sum_{i=0}^{N} s_i v_i. \tag{18}$$

Taking the limit as the segment lengths and the azimuth angle approach zero gives the result (see equation 13)

$$J^{\perp} = \left.\frac{\partial y}{\partial \phi}\right|_{\phi=0} = \frac{\sin(\theta_0)}{v_0} \int_0^s v(s)\mathrm{d}s, \tag{19}$$

where the integral is along the ray from the source location to the receiver location.

Extension to Curved Rays

The derivation of $J^{\perp}$ in the previous section that resulted in equation (19) assumes a straight ray at normal incidence to a layered material structure. To extend the result to curved rays, it must be shown that equation (16) is still valid if the x and z components of the surface normals of the velocity layers are allowed to vary arbitrarily.

Equating the x or z components of equation (4) gives

$$\frac{\sin(\theta_1)\sin(\mathrm{d}\phi_1)}{v_1} = \frac{\sin(\theta_2)\sin(\mathrm{d}\phi_2)}{v_2}. \tag{20}$$

For small $\mathrm{d}\phi$, this simplifies to

$$\frac{\sin(\theta_1)\mathrm{d}\phi_1}{v_1} = \frac{\sin(\theta_2)\mathrm{d}\phi_2}{v_2}. \tag{21}$$

Substituting equation (14) into equation (21) again produces equation (16). Therefore, the angle (in the plane) at which a ray hits a velocity interface does not affect how far the ray rises out of the plane (for small $\mathrm{d}\phi$). Thus, the derivation that resulted in equation (19) also applies to curved rays in a 2.5D medium.

Paraxial Computation of $J^{\perp}$

In this section we use the paraxial ray method to analytically derive $J^{\perp}$. The approach follows that of Virieux and Farra (1991), but extra attention is payed to the perturbations of the ray take-off parameters so that the ray Jacobian can be computed precisely. The notation largely mirrors that of Virieux and Farra (1991) and Farra and Madariaga (1987).

We start by defining a Hamiltonian,

$$H(\mathbf{x},\mathbf{p}) = \frac{1}{2}[\mathbf{p}\cdot\mathbf{p} - u^2(\mathbf{x})], \tag{22}$$

that is constructed directly from the eikonal equation,

$$|\nabla T|^2 = \frac{1}{v^2} = u^2, \tag{23}$$

where u is the slowness of the medium (v is velocity) and $\mathbf{p} = \nabla T$. The vector $\mathbf{p}$ is also referred to as slowness. Governing differential equations for rays can be derived from equation (22) using the method of characteristics and can be found in Virieux and Farra (1991). The rays are parameterized curves in six-dimensional phase space described by the vector $\mathbf{y}_0^T(\sigma) = [\mathbf{x}_0(\sigma), \mathbf{p}_0(\sigma)]$, where $\mathbf{x}_0$ is the parameterized position and the subscript indicates that this is a reference ray. There are a several common options for parameterizing the position on the ray (Červený, 2001, pp. 126). Here we choose σ (τ in Virieux and Farra, 1991), which is defined by

$$\mathrm{d}T = \mathbf{p}\cdot\mathrm{d}\mathbf{x} = u^2(\mathbf{x})\mathrm{d}\sigma. \tag{24}$$

Paraxial rays are perturbations of the reference ray and are defined by $\mathbf{x}(\sigma) = \mathbf{x}_0(\sigma) + \delta\mathbf{x}(\sigma)$ and $\mathbf{p}(\sigma) = \mathbf{p}_0(\sigma) + \delta\mathbf{p}(\sigma)$. The perturbations along the central ray, $\delta\mathbf{y}^T = (\delta\mathbf{x}, \delta\mathbf{p})$, are governed by another set of differential equations (Virieux and Farra, 1991),

$$\frac{\mathrm{d}\delta\mathbf{y}}{\mathrm{d}\sigma} = \mathbf{A}\delta\mathbf{y}, \tag{25}$$

where

$$\mathbf{A} = \begin{bmatrix} \nabla_x\nabla_p H & \nabla_p\nabla_p H \\ -\nabla_x\nabla_x H & -\nabla_p\nabla_x H \end{bmatrix}. \tag{26}$$

Additionally, the paraxial rays must satisfy

$$\delta H = \nabla_p H\cdot\delta\mathbf{p} + \nabla_x H\cdot\delta\mathbf{x} = 0, \tag{27}$$

otherwise, the computed trajectories are not actually rays. If this condition is satisfied anywhere on a paraxial ray, then it is satisfied everywhere on that ray.

To compute the ray Jacobian, we start by perturbing the slowness, $\mathbf{p}$, at the start of the central ray to find two new paraxial rays. These two new rays define the cross-sectional area of the ray tube. In order to find a Jacobian per solid angle, we must ensure that our perturbations trace out a known portion of a solid angle.

To satisfy equation (27) at the start of the paraxial ray, we must ensure that the perturbations of initial slowness for the two paraxial rays, $\delta\mathbf{p}_i$ and $\delta\mathbf{p}_i'$, are perpendicular to the initial slowness, $\mathbf{p}_i$. We are not perturbing the starting position of the ray, only the take-off angle, so $\delta\mathbf{x}_i = 0$. Further, if we ensure that each perturbation is of length $\epsilon|\mathbf{p}_i|$, where ϵ is a small positive number and the perturbations are perpendicular to each other, then they trace out an area of $\epsilon^2|\mathbf{p}_i|^2$ on a sphere of radius $|\mathbf{p}_i|$. This corresponds to a solid angle of ϵ^2 steradians. Requiring that the perturbations are perpendicular to each other and are of the same length is not essential, but doing so simplifies the computation of the solid angle spanned by the rays. If we define the position perturbations associated with the slowness perturbations $\delta\mathbf{p}_i$ and $\delta\mathbf{p}_i'$ to be $\delta\mathbf{x}$ and $\delta\mathbf{x}'$, respectively, then we can express the ray Jacobian per solid angle J_{3D}^{Ω} as

$$\epsilon^2 J_{3D}^{\Omega} = \hat{\mathbf{p}}\cdot(\delta\mathbf{x}\times\delta\mathbf{x}'), \tag{28}$$

where we have assumed that $\delta\mathbf{p}_i\times\delta\mathbf{p}_i'$ is in the direction of $\mathbf{p}_i$ rather than $-\mathbf{p}_i$. This ensures that the sign of the Jacobian is compatible with the geometrical derivation (i.e., positive for a uniform medium).

A set of initial perturbations that satisfies these requirements is

$$\delta\mathbf{p}_i = \epsilon\frac{|\mathbf{p}_i|}{\sqrt{p_{zi}^2 + p_{yi}^2}}(0, -p_{zi}, p_{yi}), \tag{29}$$

and

$$\delta\mathbf{p}_i' = \epsilon\frac{|\mathbf{p}_i|}{\sqrt{(p_{yi}^2 + p_{zi}^2)^2 + p_{xi}^2(p_{yi}^2 + p_{zi}^2)}} \times (-p_{yi}^2 - p_{zi}^2, p_{xi}p_{yi}, p_{xi}p_{zi}). \tag{30}$$

Following Virieux and Farra (1991), we choose three reference paraxial trajectories with unit perturbations of initial slowness in each coordinate direction:

$$\delta\mathbf{p}_1 = (1,0,0), \tag{31}$$

$$\delta\mathbf{p}_2 = (0,1,0), \tag{32}$$

and

$$\delta\mathbf{p}_3 = (0,0,1). \tag{33}$$

The corresponding perturbations in position along each trajectory are $\delta\mathbf{q}_1$, $\delta\mathbf{q}_2$, and $\delta\mathbf{q}_3$. In general, the trajectories are not rays because equation (27) is not satisfied. However, the perturbations in equation (28) for the two paraxial rays, $\delta\mathbf{x}$ and $\delta\mathbf{x}'$, can be constructed using linear combinations of these three trajectories. This allows equation (28) to be expressed as a determinant (Virieux and Farra, 1991):

$$J^{\Omega}_{3D} = \frac{-|\mathbf{p}_i|}{|\mathbf{p}|}\begin{vmatrix} p_x & \delta q_{1x} & \delta q_{2x} & \delta q_{3x} \\ p_y & \delta q_{1y} & \delta q_{2y} & \delta q_{3y} \\ p_z & \delta q_{1z} & \delta q_{2z} & \delta q_{3z} \\ 0 & p_{xi} & p_{yi} & p_{zi} \end{vmatrix}. \tag{34}$$

Using analogous reasoning, we can express the 2D ray Jacobian as

$$J_{2D} = \frac{1}{|\mathbf{p}|}\begin{vmatrix} p_x & \delta q_{1x} & \delta q_{3x} \\ p_z & \delta q_{1z} & \delta q_{3z} \\ 0 & p_{xi} & p_{zi} \end{vmatrix}, \tag{35}$$

where $\mathbf{p}$ has no y component.

In the 2.5D case the material properties do not vary in the y direction. The paraxial raytracing equation (25) can then be simplified and expressed as

$$\frac{\mathrm{d}}{\mathrm{d}\sigma}\begin{bmatrix} \delta q_x \\ \delta q_y \\ \delta q_z \\ \delta p_x \\ \delta p_y \\ \delta p_z \end{bmatrix} = \begin{bmatrix} 0 & 0 & 0 & 1 & 0 & 0 \\ 0 & 0 & 0 & 0 & 1 & 0 \\ 0 & 0 & 0 & 0 & 0 & 1 \\ \frac{1}{2}\frac{\partial^2 u^2}{\partial x^2} & 0 & \frac{1}{2}\frac{\partial^2 u^2}{\partial x \partial z} & 0 & 0 & 0 \\ 0 & 0 & 0 & 0 & 0 & 0 \\ \frac{1}{2}\frac{\partial^2 u^2}{\partial x \partial z} & 0 & \frac{1}{2}\frac{\partial^2 u^2}{\partial z^2} & 0 & 0 & 0 \end{bmatrix}\begin{bmatrix} \delta q_x \\ \delta q_y \\ \delta q_z \\ \delta p_x \\ \delta p_y \\ \delta p_z \end{bmatrix}. \tag{36}$$

Inspection of equation (36) indicates that the y component of the slowness vector is a constant along the ray:

$$\frac{\mathrm{d}\delta p_y}{\mathrm{d}\sigma} = 0. \tag{37}$$

Additionally, from equation (36), we can relate the y component of the position perturbation to the perturbation of initial slowness by solving

$$\frac{\mathrm{d}\delta q_y}{\mathrm{d}\sigma} = \delta p_y \tag{38}$$

to obtain

$$\delta q_y = \delta p_y \sigma. \tag{39}$$

From equation (39), we see that $\delta q_{2y} = \sigma$ and $\delta q_{1y} = \delta q_{3y} = 0$, thus allowing us to simplify the second row of equation (34). Similarly, $\delta q_{2x} = \delta q_{2z} = 0$. The 3D Jacobian (34) can now be simplified to:

$$J^{\Omega}_{3D} = \frac{-|\mathbf{p}_i|}{|\mathbf{p}|}\begin{vmatrix} p_x & \delta q_{1x} & 0 & \delta q_{3x} \\ p_y & 0 & \sigma & 0 \\ p_z & \delta q_{1z} & 0 & \delta q_{3z} \\ 0 & p_{xi} & p_{yi} & p_{zi} \end{vmatrix}. \tag{40}$$

This can be manipulated and expressed in a form that contains the determinant of the 2D ray Jacobian (35),

$$J^{\Omega}_{3D} = \sigma\frac{|\mathbf{p}_i|}{|\mathbf{p}|}\mathrm{Det}_{2D} - p^2_{yi}\frac{|\mathbf{p}_i|}{|\mathbf{p}|}\begin{vmatrix} \delta q_{1x} & \delta q_{3x} \\ \delta q_{1z} & \delta q_{3z} \end{vmatrix}, \tag{41}$$

where Det_{2D} is the determinant in equation (35), and we have made use of equation (37). The vector $\mathbf{p}$ in equation (35) does not have a y component, so it would not be correct to include J_{2D} in equation (41). However, if we set $p_{yi} = 0$, as is the case for planar rays, we can write

$$J^{\Omega}_{3D} = \sigma|\mathbf{p}_i|J_{2D}. \tag{42}$$

The 3D Jacobian can be factored into a parallel and perpendicular part. The parallel part is simply the 2D Jacobian, and the perpendicular part is

$$J^{\Omega\perp} = \sigma|\mathbf{p}_i| = \frac{1}{v_0}\int_0^s v(s)\mathrm{d}s, \tag{43}$$

where s is arc length along the ray, and v_0 is the velocity at the start of the ray. The definition of the ray parameter (24) has been used to express σ as an integral, and the eikonal equation (23) gives us $|\mathbf{p}_i| = 1/v_0$.

We can use the solid-angle relationship $\mathrm{d}\Omega = \sin(\theta)\mathrm{d}\theta\mathrm{d}\phi$ to convert the solid-angle Jacobian J^{Ω}_{3D} into J_{3D} that operates on perturbations of the spherical coordinates $\mathrm{d}\theta$ and $\mathrm{d}\phi$,

$$J_{3D} = \sin(\theta_0)J^{\Omega}_{3D}, \tag{44}$$

or

$$J^{\perp} = \frac{\sin(\theta_0)}{v_0}\int_0^s v(s)\mathrm{d}s, \tag{45}$$

which is identical to equation (19), thus verifying the geometrical derivation.

Simplified Transfer Function

Incorporating equations (10), (11), and (19) or (43) into equation (1) results in the simplified expression

$$TF = -i\pi H^{(2)}_0[\omega T(s)]e^{i\omega T(s)}\sqrt{T(s)\int_0^s v(s)\mathrm{d}s}. \tag{46}$$

If we replace the Hankel function in equation (46) with its large-argument expansion (Abramowitz and Stegun, 1964, pp. 364), we obtain

$$TF \approx e^{-i\frac{\pi}{4}}\sqrt{\frac{1}{f}\int_0^s v(s)\mathrm{d}s}. \tag{47}$$

Although equation (46) can be used, equation (47) provides accurate results when the source and receiver are sufficiently far apart.

Conclusion

The perpendicular portion, $J^{\perp}$, of the ray Jacobian, J, was derived for the 2.5D planar ray case through a graphical approach and confirmed by an analytical approach. Both approaches are reasonably straightforward and produce the same result, but the graphical approach requires only a knowledge of Snell's law. It also provides a more physically intuitive view of ray spreading out of the plane and the factorizability of the ray Jacobian.

Data and Resources

No data were collected or used in this article. The article was prepared in LaTeX, and the figures were created with Inkscape. Maple was used to verify some of the equations.

Acknowledgments

The authors would like to thank the National Science and Engineering Research Council of Canada for its direct financial support. This work has also been partially supported by the French Agence Nationale de la Recherche under Grant ANR-2011-BS56-017.

References

Abramowitz, M., and I. A. Stegun (1964). *Handbook of Mathematical Functions with Formulas, Graphs, and Mathematical Tables*, U.S. Government Printing Office, 10th printing, December 1972 with corrections, Washington, D.C., 1046 pp.

Bleistein, N. (1986). Two-and-one-half dimensional in-plane wave propagation, *Geophys. Prospect.* **34,** no. 5 686–703.

Červený, V. (2001). *Seismic Ray Theory.* Cambridge University Press, New York, 724 pp.

Červený, V., and F. Hron (1980). The ray series method and dynamic ray tracing system for three-dimensional inhomogeneous media, *Bull. Seismol. Soc. Am.* **70,** no. 1 47–77.

Červený, V., and R. Ravindra (1971). *Theory of Seismic Head Waves*. University of Toronto Press, Toronto, Ontario, Canada, 312 pp.

Farra, V., and R. Madariaga (1987). Seismic waveform modeling in heterogeneous media by ray perturbation theory, *J. Geophys. Res.* **92,** no. B3 2697–2712.

Virieux, J., and V. Farra (1991). Ray tracing in 3-D complex isotropic media: An analysis of the problem, *Geophysics* **56,** no. 12 2057–2069.

Yedlin, M. (1987). Uniform asymptotic solution for the Green's function for the two-dimensional acoustic equation, *J. Acoust. Soc. Am.* **81,** 238–243.

Yedlin, M., D. Van Vorst, and J. Virieux (2012). Uniform asymptotic conversion of Helmholtz data from 3D to 2D, *J. Appl. Geophys.* **78,** 2–8.

Department of Electrical and Computer Engineering
University of British Columbia
2332 Main Mall
Vancouver, B.C., Canada V6T 1Z4
darylv@ece.ubc.ca
(D.V., M.J.Y.)

Institut des Sciences de la Terre—ISTerre
Université de Grenoble I
CNRS, BP 53
38041 Grenoble CEDEX 9
France
(J.V.)

Manuscript received 7 February 2012